Electronic Supplementary Material (ESI) for Lab on a Chip.

Supporting Information

Real-time continuous monitoring of dynamic concentration profiles studied with biosensing by particle motion

Max H. Bergkamp[1,3], Sebastian Cajigas[4], Leo J. van IJzendoorn[2,3], Menno W.J. Prins[1,2,3,4*]

[1]Department of Biomedical Engineering, Eindhoven University of Technology, 5612 AE Eindhoven, The Netherlands
[2]Department of Applied Physics and Science Education, Eindhoven University of Technology, 5612 AE Eindhoven, The Netherlands
[3]Institute for Complex Molecular Systems (ICMS), Eindhoven University of Technology, 5612 AE Eindhoven, The Netherlands
[4]Helia Biomonitoring, 5612 AR Eindhoven, The Netherlands
*Email: m.w.j.prins@tue.nl

S1. Experimental setup

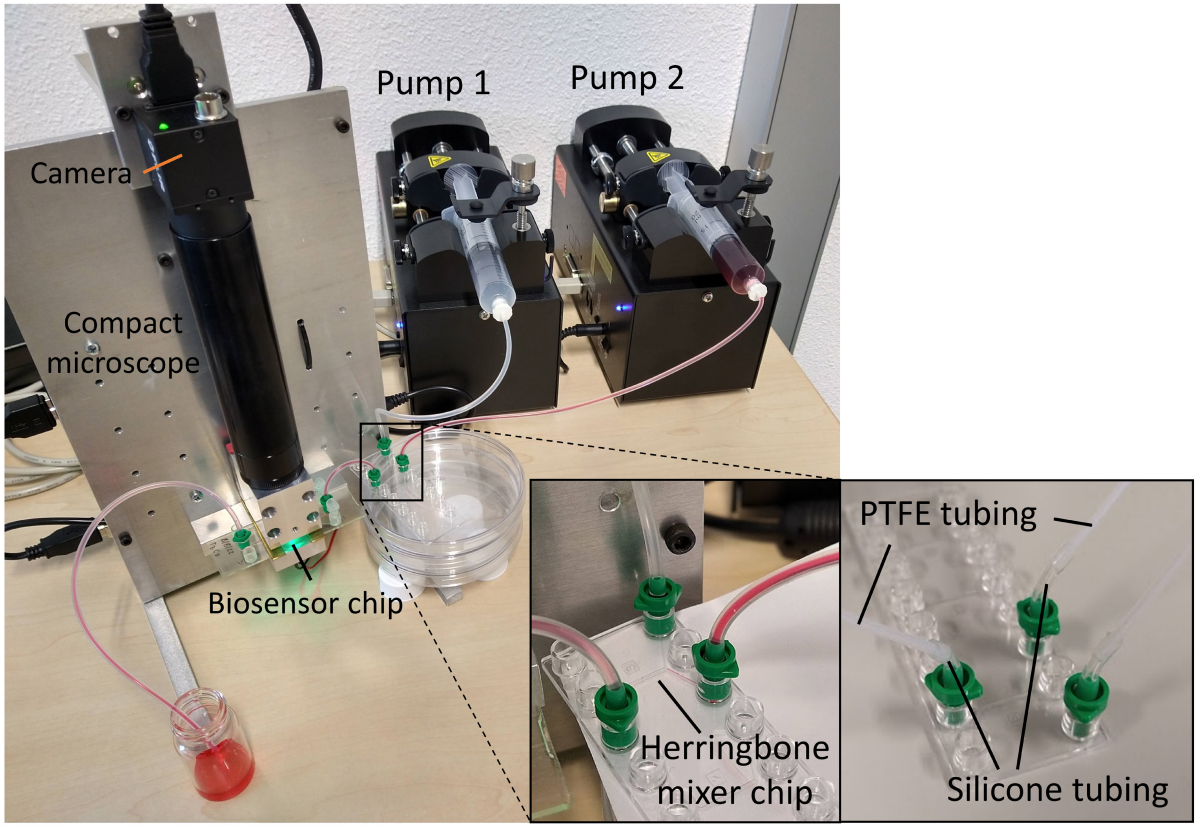

Figure S1. Picture of the setup for generating and measuring dynamic concentration profiles. The flow rates of pump 1 (containing a low concentration) and pump 2 (containing a high concentration) are continuously controlled by a computer. The output solutions of pump 1 and pump 2 are mixed in a herringbone mixer chip to generate dynamic concentration profiles. The output of the herringbone mixer chip is connected to the biosensor chip that is imaged with a compact brightfield microscopy setup. The images captured by the camera are processed in real time. The setup was equipped with soft silicone tubing in earlier experiments (as shown in the picture of the complete setup). In order to prevent the formation of air bubbles we switched to PTFE tubing, which was connected to the Luer connectors with small parts of silicone tubing (see inset on the right); the presented experiments were all performed with the PTFE tubing.

S2. Diffusion coefficient

The mean squared displacement (MSD) in two dimensions can be calculated experimentally from the x and y time traces of a single particle. The MSD for a time lag t_{lag} of m datapoints in a window of w datapoints is given by[1]:

$$MSD_w(t_{lag} = m \cdot dt) = \frac{1}{w-m} \sum_{i=1}^{w-m} ([x(i+m) - x(i)]^2 + [y(i+m) - y(i)]^2) \quad \text{(S1)}$$

where dt is the time between consecutive datapoints and is equal to the reciprocal of the frame rate.

For a particle that moves according to Brownian motion in two dimensions, the MSD scales linearly with the time lag according to[1,2]:

$$MSD(t_{lag}) = 4Dt_{lag} \quad \text{(S2)}$$

The diffusion coefficient can be derived from the MSD as follows:

$$D = \frac{MSD(t_{lag})}{4 \cdot t_{lag}} = \frac{MSD(m \cdot dt)}{4 \cdot m \cdot dt} \quad \text{(S3)}$$

The diffusion coefficient D_w in a moving average window of w datapoints ($w = 60$ datapoints in the presented data) is determined from a weighted average of the diffusion coefficients for multiple time lags (m = {1,10}):

$$D_w = \sum_{m=1}^{10} \left(\frac{\omega_m}{\sum_{m=1}^{10} \omega_m} \cdot \frac{MSD_w(m \cdot dt)}{4 \cdot m \cdot dt} \right) \quad \text{(S4)}$$

The weight factors for each time lag ω_m are chosen as the reciprocal of the relative variance of the MSD[3]:

$$\omega_m = \frac{w - m + 1}{m(2m^2 + 1)} \quad \text{(S5)}$$

S3. Real-time cortisol sensing with BPM

S3.1 Motion patterns

Figure S2 shows the motion patterns of individual particles that were recorded at different cortisol concentrations.

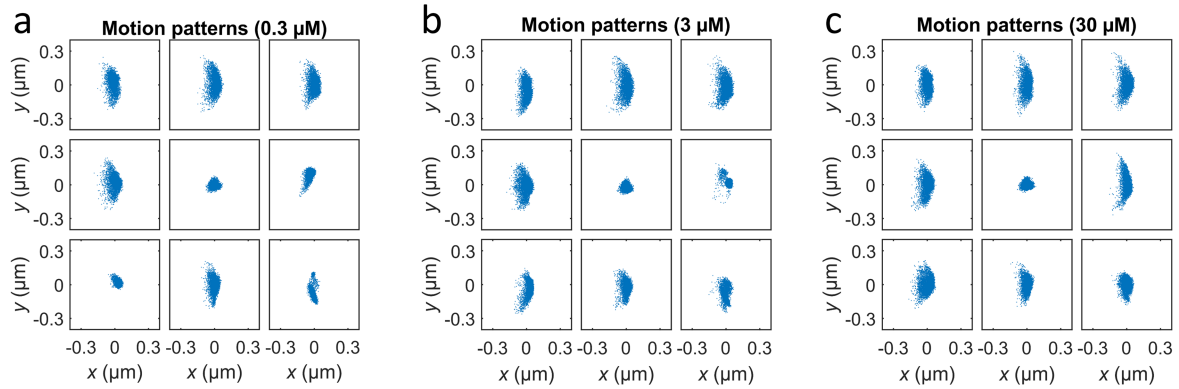

Figure S2. Motion patterns of 9 individual particles, shown at different cortisol concentrations, for a fluid flow rate of 100 µL/min. Motion patterns are x and y scatter plots of the localized particle positions in a measurement block of 30 seconds. (a) 0.3 µM. (b) 3 µM. (c) 30 µM.

S3.2 Repeatability

Figure S3 shows a bar chart of the average bound fraction of the baseline concentration (0.3 µM) after applying multiple concentration steps at higher cortisol concentrations. The standard deviation of the four repetitions in the bound fraction is ~0.011, which is ~5% relative to the maximum signal change of the dose-response relationship of 0.217 (see Table S2). These measurements show a stable signal at the baseline concentration for timescales up to 1 hour. Section S5 discusses signal changes on longer timescales and a method to take account of such changes.

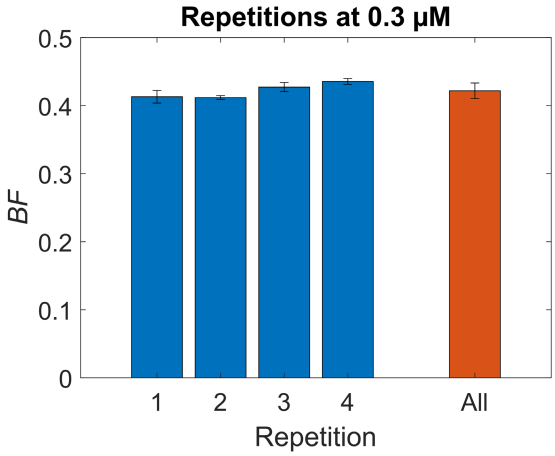

Figure S3. Bound fraction at the baseline concentration of 0.3 µM. The bound fraction value of each of the four repetitions (blue) is determined from the bound fraction values of 10 consecutive measurement blocks of 30 seconds. The red bar is the average bound fraction of the four repetitions. The error bars indicate the standard deviation.

S3.3 Single-exponential fits

Figure S4 shows the single-exponential fits that were performed on data with a 10 times higher time resolution compared to main Figure 4a. Each measurement block of 30 seconds was split into 10 sub-blocks of 3 seconds. This approach results in a larger number of datapoints for each fit, which was done to reduce uncertainty, i.e., to achieve narrower confidence intervals of the fitted coefficients.

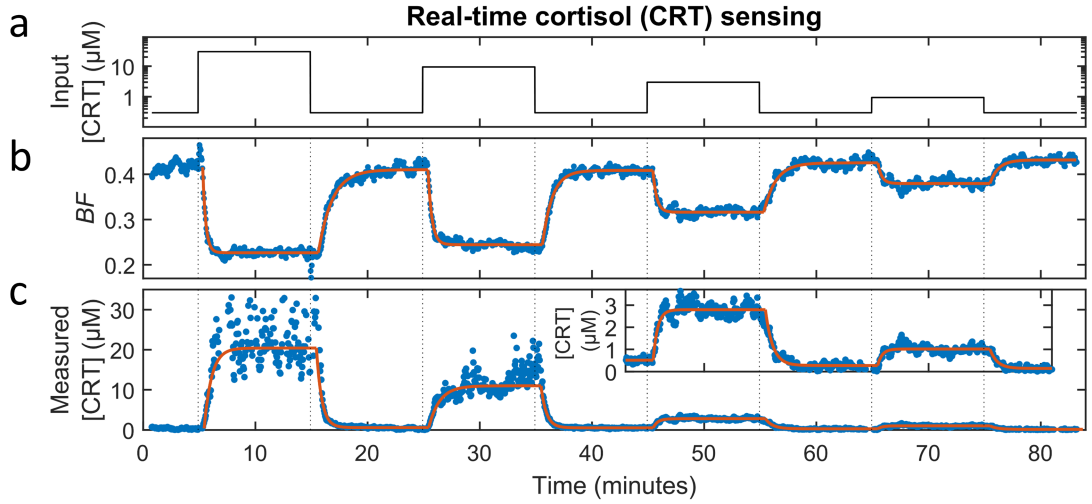

Figure S4. Single-exponential fitting on experimental data with a higher time resolution. (a) Real-time sensing of cortisol concentrations with BPM. (a) Cortisol concentration as a function of time generated by controlled microfluidic mixing. (b) Bound fraction as a function of time with a 10 times higher time resolution compared to the data presented in main Figure 4a, which was obtained by splitting each measurement block of 30 seconds into 10 sub-blocks of 3 seconds (post-processing). Datapoints were fitted with single-exponential curves to extract equilibrium bound fraction values that were needed to construct the dose-response curve (main Figure 4b). (c) Measured cortisol concentration as a function of time. The measured cortisol concentration was derived from the signal and the fitted dose-response relationship. Datapoints were fitted with single-exponential curves to extract the transport time delay and the characteristic equilibration time (main Figure 4c).

S4. Time delay contributions

Table S1 gives an overview of the characteristic physicochemical and signal processing times that contribute to the total time delay of the BPM cortisol sensor. These estimations indicate that advection and diffusion are the most significant contributors to the total time delay of the real-time cortisol sensor.

Table S1. Estimations of the characteristic physicochemical and signal processing times that contribute to the total time delay of the BPM cortisol sensor. The characteristic advection and diffusion times were estimated based on the measurement chamber and tubing dimensions; the characteristic reaction time was estimated based on dissociation rates measured in previous BPM cortisol sensors. The transport time delay and characteristic equilibration time were determined from the presented experimental data in main Figure 4. The signal processing time delay includes the block size and the analysis time; the analysis time was saved in the log files of the real-time signal processing software.

Physico-chemical processes	Characteristic time	Parameter values (BPM cortisol sensor)	Time (s)	**BPM cortisol sensor:** Transport time delay: $\Delta t_{0,BPM} \approx 32\ s$ Characteristic equilibration time: $\tau_{C,BPM} \approx 37\ s$ Total physicochemical time delay: $\Delta t_{C63\%} = \Delta t_{0,BPM} + \tau_{C,BPM} \approx 70\ s$	Total time delay of the real-time sensor: $\Delta t_{RTS} = \Delta t_{C63\%} + \Delta t_{SP}$ BPM cortisol sensor: $\Delta t_{RTS} \approx 90\ s$
Advection	$\tau_A = V/Q$ (ref.[4]) V: Swept volume (tubing and measurement chamber) Q: Flow rate	$V \sim$ 50-100 µL V_{tubing}= 25 µL $V_{chamber}$= 60 µL Q = 100 µL/min	30-60		
Diffusion	$\tau_D = d^2/D$ (ref.[4]) d: Typical distance of analyte diffusion D: Diffusion coefficient	$d_y \sim$ 100-200 µm $h_{chamber}$= 400 µm $D_{CRT} \sim 3{\cdot}10^{-10}$ m^2 s^{-1} (ref.[5])	30-130		
Reaction	$\tau_R = (k_{on}C + k_{off})^{-1}$ (ref.[4]) so $\tau_R < {k_{off}}^{-1}$ k_{off}: dissociation rate constant	$k_{off} \sim 0.03$ s^{-1} (ref.[6])	<30		
Signal processing	Parameter		Time (s)	Signal processing time delay: $\Delta t_{SP} = \frac{t_{block}}{2} + t_{analysis}$ $\Delta t_{SP} \approx 20\ s$	
Data sampling	t_{block}: Block size in real-time sensing experiment		30		
Processing	$t_{analysis}$: Time difference between the end of the measurement block and the reporting of the measurement signal corresponding to that block		2-3		

S5. Time-dependent dose-response relationship

The dose-response relationship of the cortisol sensor shows long term changes, e.g., due to release of molecules from particle or substrate, or due to non-specific interactions[7]. As a first-order correction, we assume a time-dependent dose-response relationship with time-dependent maximum and minimum signal levels and constant EC_{50} and n:

$$S(t) = S_{min}(t) + \frac{S_{max}(t) - S_{min}(t)}{1 + \left(\frac{C}{EC_{50}}\right)^{n}} \quad \text{(S6)}$$

Calibration measurements were performed before ($t = t_1$) and after ($t = t_2$) the sinusoidal modulations, by applying concentration step functions of 300 nM and 6 µM and by measuring the equilibrium bound fraction (see Fig. S5b). Table S2 gives the fit coefficients that were determined from the calibration measurements by fitting the data with Eq. S6. Linear interpolation was performed to determine a time-dependent S_{min} and S_{max}.

Table S2. Dose-response relationship coefficients as a function of time.

Coefficient	Main Fig. 4b	$t = t_1$	$t = t_2$	$t_1 < t < t_2$: Linear interpolation
$S_{min}(t)$	0.215	0.266	0.296	$S_{min}(t_1) + (t - t_1) \cdot \frac{S_{min}(t_2) - S_{min}(t_1)}{(t_2 - t_1)}$
$S_{max}(t)$	0.432	0.443	0.455	$S_{max}(t_1) + (t - t_1) \cdot \frac{S_{max}(t_2) - S_{max}(t_1)}{(t_2 - t_1)}$
EC_{50}	2.52	2.52	2.52	2.52
n	1.27	1.27	1.27	1.27

Figure S5c shows the effect of applying the time-dependent dose-response relationship for calculating measured analyte concentrations.

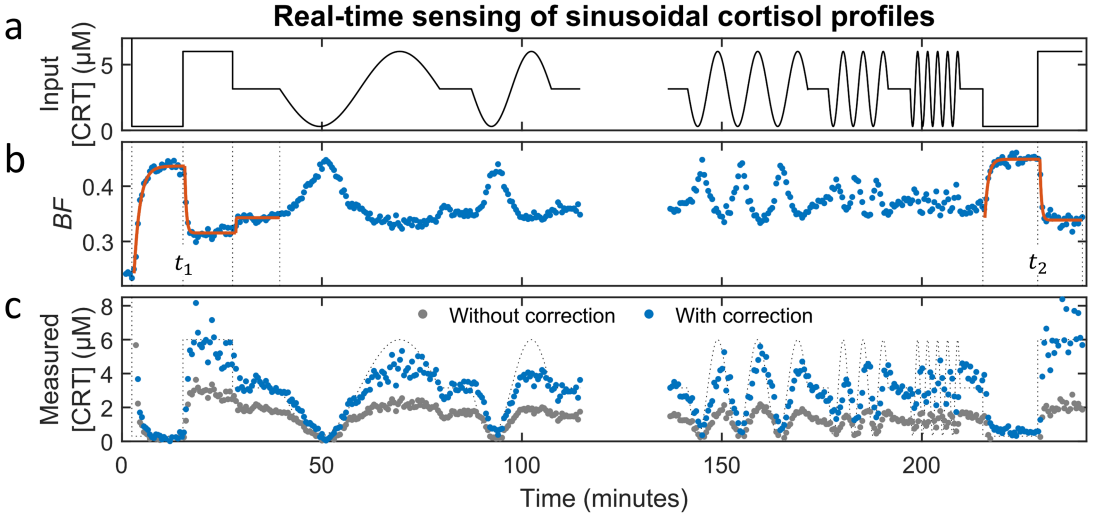

Figure S5. Correction of the dose-response relationship. (a) Cortisol concentration as a function of time that was generated by controlled microfluidic mixing. (b) Bound fraction as a function of time. Datapoints were fitted with single-exponential functions (red curves) to extract equilibrium bound fraction values that were needed for calibration. (c) Measured cortisol concentration as a function of time. The measured cortisol concentration without correction was derived from the fitted dose-response relation in main Figure 4b. The corrected measured cortisol concentration was derived from the time-dependent dose-response relationship (see Eq. S6 and Table S2).

S6. Model of an advection-limited measurement chamber

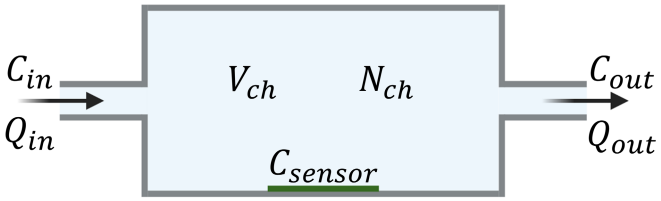

Figure S6. Model of an advection-limited measurement chamber.

Assume a measurement chamber with volume V_{ch}. The flowrate at the outlet Q_{out} is equal to the flowrate at the inlet Q_{in}:

$$Q_{in} = Q_{out} = Q \tag{S7}$$

We assume perfect mixing in the chamber, i.e., a homogeneous analyte concentration C_{ch} in the measurement chamber:

$$C_{ch} = \frac{N_{ch}}{V_{ch}} = C_{sensor} = C_{out} \tag{S8}$$

with N_{ch} the number of analyte molecules in the measurement chamber. The time derivative of the output concentration can be expressed as:

$$\frac{dC_{out}}{dt} = \frac{1}{V_{ch}}\frac{dN_{ch}}{dt} = \frac{Q(C_{in} - C_{out})}{V_{ch}} \tag{S9}$$

In an experiment with a sinusoidal concentration modulation, we assume a time-dependent input concentration $C_{in}(t)$ with angular frequency ω and amplitude ΔC_{in}. The time-dependent output concentration $C_{out}(t)$ has the same frequency:

$$C_{in}(t) = \Delta C_{in} e^{i\omega t} \tag{S10}$$

$$C_{out}(t) = \Delta C_{out} e^{i\omega t} \tag{S11}$$

The time derivative of Eq. S11 is:

$$\frac{dC_{out}}{dt} = i\omega \Delta C_{out} e^{i\omega t} \tag{S12}$$

Combining Eqs. S9-S12 and dividing by $e^{i\omega t}$ gives:

$$i\omega \Delta C_{out} = \frac{Q(\Delta C_{in} - \Delta C_{out})}{V_{ch}} \tag{S13}$$

Rewriting this equation allows to express the transfer function H:

$$H = \frac{\Delta C_{out}}{\Delta C_{in}} = \frac{1}{1 + \frac{i\omega V_{ch}}{Q}} \tag{S14}$$

The absolute value of H equals the transfer magnitude:

$$|H| = \frac{1}{\sqrt{1 + \left(\frac{\omega V_{ch}}{Q}\right)^2}} = \frac{1}{\sqrt{1 + \left(\frac{2\pi f V_{ch}}{Q}\right)^2}} = \frac{1}{\sqrt{1 + \left(\frac{f}{f_c}\right)^2}} \tag{S15}$$

with cutoff frequency f_c:

$$f_c = \frac{Q}{2\pi V_{ch}} \tag{S16}$$

The cutoff frequency relates to the advective refresh rate of the fluid in the measurement chamber. A flow rate of 100 µL/min and chamber volume of 60 µL give a cutoff frequency of 4.4 mHz.

References

1. Manzo, C. & Garcia-Parajo, M. F. A review of progress in single particle tracking: from methods to biophysical insights. *Reports Prog. Phys.* **78**, 124601 (2015).
2. Metzler, R., Jeon, J. H., Cherstvy, A. G. & Barkai, E. Anomalous diffusion models and their properties: Non-stationarity, non-ergodicity, and ageing at the centenary of single particle tracking. *Phys. Chem. Chem. Phys.* **16**, 24128–24164 (2014).
3. Huet, S. *et al.* Analysis of transient behavior in complex trajectories: Application to secretory vesicle dynamics. *Biophys. J.* **91**, 3542–3559 (2006).
4. Lubken, R. M., de Jong, A. M. & Prins, M. W. J. Real-Time Monitoring of Biomolecules: Dynamic Response Limits of Affinity-Based Sensors. *ACS Sensors* **7**, 286–295 (2022).
5. Lee, M. A., Bakh, N., Bisker, G., Brown, E. N. & Strano, M. S. A Pharmacokinetic Model of a Tissue Implantable Cortisol Sensor. *Adv. Healthc. Mater.* **5**, 3004–3015 (2016).
6. van Smeden, L. *et al.* Reversible Immunosensor for the Continuous Monitoring of Cortisol in Blood Plasma Sampled with Microdialysis. *ACS Sensors* **7**, 3041–3048 (2022).
7. Lin, Y. T., Vermaas, R., Yan, J., De Jong, A. M. & Prins, M. W. J. Click-Coupling to Electrostatically Grafted Polymers Greatly Improves the Stability of a Continuous Monitoring Sensor with Single-Molecule Resolution. *ACS Sensors* **6**, 1980–1986 (2021).